HHS Public Access

Author manuscript

Cell Signal. Author manuscript; available in PMC 2020 October 01.

Published in final edited form as:

Cell Signal. 2019 October ; 62: 109349. doi:10.1016/j.cellsig.2019.109349.

Intramolecular Electrostatic Interactions Contribute to Phospholipase Cβ3 Autoinhibition

Candi M. Esquina[1,†], **Elisabeth E. Garland-Kuntz**[2], **Daniel Goldfarb**[1], **Emily K. McDonald**[3], **Brianna N. Hudson**[2], **Angeline M. Lyon**[1,2,*]

[1]Department of Chemistry, Purdue University, West Lafayette, IN 47906

[2]Department of Biological Sciences, Purdue University, West Lafayette, IN 47906

[3]Department of Toxicology, Purdue University, West Lafayette, IN 47906

Abstract

Phospholipase Cβ (PLCβ) enzymes regulate second messenger production following the activation of G protein-coupled receptors (GPCRs). Under basal conditions, these enzymes are maintained in an autoinhibited state by multiple elements, including an insertion within the catalytic domain known as the X–Y linker. Although the PLCβ X–Y linker is variable in sequence and length, its C-terminus is conserved and features an acidic stretch, followed by a short helix. This helix interacts with residues near the active site, acting as a lid to sterically prevent substrate binding. However, deletions that remove the acidic stretch of the X–Y linker increase basal activity to the same extent as deletion of the entire X–Y linker. Thus, the acidic stretch may be the linchpin in autoinhibition mediated by the X–Y linker. We used site-directed mutagenesis and biochemical assays to investigate the importance of this acidic charge in mediating PLCβ3 autoinhibition. Loss of the acidic charge in the X–Y linker increases basal activity and decreases stability, consistent with loss of autoinhibition. However, introduction of compensatory electrostatic mutations on the surface of the PLCβ3 catalytic domain restore activity to basal levels. Thus, intramolecular electrostatics modulate autoinhibition by the X–Y linker.

Keywords

Phospholipase C; calcium; phosphatidylinositol lipids; signaling proteins; signal transduction; regulation; electrostatics

*To whom correspondence should be addressed: Depts. of Chemistry and Biological Sciences, Purdue University, 560 Oval Dr., West Lafayette, IN 47907. Tel.: 765-494-5291; lyonam@purdue.edu.

†C.M.E.: Albany Molecular Research, Inc., 26 Corporate Circle, Buffalo, New York 12203

Author Contributions

A.M.L. designed the overall experimental approach. C.M.E, E.E.G., D. G.‡, and E.K.M.‡ cloned, expressed, and purified PLCβ3-Δ847 and all variants. B.N.H. expressed and purified PLCβ3 and PLCβ3 PLCβ3-Δ892. C.M.E. performed DSF assays, and C.M.E. and E.E.G.-K. performed the activity and liposome binding assays. The manuscript was written through contributions of all authors. All authors have given approval to the final version of the manuscript. ‡These authors contributed equally.

Introduction

Phospholipase Cβ (PLCβ) enzymes are members of the highly-conserved PLC family, which canonically hydrolyze phosphatidylinositol-4,5-bisphosphate (PIP_2) at the plasma membrane to produce inositol-1,4,5-triphosphate (IP_3) and diacylglycerol (DAG). These second messengers increase intracellular Ca^{2+} and activate protein kinase C (PKC), thereby regulating cell proliferation, differentiation, and survival[4]. PLCβ enzymes have low basal activity and are activated through direct interactions with the heterotrimeric G protein subunits $G\alpha_q$ and $G\beta\gamma$, linking PLCβ activation to G protein-coupled receptor (GPCR) stimulation[4, 5]. The function of PLCβγenzymes has been best characterized in the cardiovascular system, where changes in expression and/or G protein-dependent activation contribute to arrhythmias[6, 7] and hypertrophy[8].

PLCβγshares a highly conserved core domain architecture with other PLC isoforms. This core consists of a pleckstrin homology (PH domain), four tandem EF hand repeats, a catalytic TIM barrel domain, and a C2 domain (Figure 1)[4, 9]. These four domains are required for lipase activity in the PLCβ subfamily[10]. The PLCβ subfamily also contains two C-terminal regulatory domains immediately following the C2 domain. The proximal C-terminal domain (CTD) contains the primary $G\alpha_q$ binding site (Hα1/Hα2)[3] and an autoinhibitory helix[11]. An unconserved linker region connects the proximal CTD to the distal CTD, which contributes to membrane binding and $G\alpha_q$-dependent activation[12–15].

PLCβγ is regulated through at least three structural elements, two of which are unique to the PLCβ subfamily[11, 14, 16–18]. The proximal CTD is proposed to stabilize a more catalytically quiescent conformational state[11, 18] and inhibit interactions between the core domains and the membrane[19]. The distal CTD also contributes to membrane binding, and may help partition the enzyme between the membrane and the cytoplasm[14, 19–21]. PLCβ is also regulated by the X–Y linker, a variable length insertion within the TIM barrel domain. The X–Y linker is found in several PLC subfamilies, and has been shown to autoinhibit the PLCβ and PLCβ3 subfamilies[4, 17]. Deletion of the entire X–Y linker increases basal activity, and in PLCβ and PLCε, decreases the efficacy of G protein-dependent activation[17, 18]. The proposed mechanism by which regulation by the X–Y linker is achieved is best understood in the context of PLCβ. The linker is largely unconserved in length and sequence, with the exception of its C-terminal region which contains a ~10–15 stretch of acidic residues followed by ~15 residues that fold into a short α helix. This helix interacts with residues adjacent to the active site, functioning as a lid to physically block substrate binding[1, 3, 11, 14, 17, 18]. Displacement of this lid helix is proposed to occur via interfacial activation, wherein unfavorable electrostatic interactions between the acidic stretch of the X–Y linker and the negatively charged membrane leaflet eject the helix to expose the active site[17].

Recent studies suggest the acidic stretch may have multiple roles in interfacial activation. Deletions that include the acidic stretch or deletion of the entire X–Y linker destabilize PLCβ to the same extent, suggesting that this region contributes to the global thermal stability of the enzyme. In addition, the crystal structure of a PLCβ3 variant lacking the acidic stretch of the X–Y linker had a disordered lid helix[18]. These observations suggest that

the acidic stretch of the X–Y linker could form stabilizing interactions with the surface of the PLCβ core, fixing the lid helix in the bound conformation observed in most crystal structures[1, 3, 11, 14, 17, 18]. In support of this hypothesis, a prior crystal structure of PLCβ2 revealed electron density for the last two residues of the acidic stretch that appear to interact with conserved basic residues on the surface of the TIM barrel domain[1]. These electrostatic interactions between the disordered acidic stretch and basic residues on the lipase domain could be sufficient for lid helix stabilization, thereby increasing thermal stability and inhibiting basal activity. Indeed, conserved basic residues on the surface of the TIM barrel are also observed in structures of PLCβ3 (Figure 1)[1, 3, 11, 14, 17, 18].

Prior studies have tried to dissect the function of the X–Y linker through deletion analysis. Herein, we sought to refine analysis of the linker by creating charge reversal mutants in human PLCβ3 to test hypotheses concerning the molecular mechanisms underlying autoregulation by the linker. For these studies, we used a C-terminal truncation of PLCβ3, PLCβ3-Δ847[11, 19], This truncation allows us to directly evaluate the role of surface charge on the catalytic core of the enzyme to basal activity, stability and liposome binding, without the confounding impact that the membrane binding distal CTD would cause. In addition, this truncation also has robust basal activity, due to the removal of the autoinhibitory proximal CTD. We purified PLCβ3-Δ847 and charge reversal mutants to homogeneity and compared their thermal stabilities, specific activities, and interactions with liposomes. PLC activity has historically been measured using a radioactivity-based liposome assay *in vitro*. However, the radiolabeled [^{3}H]-PIP_2 substrate is no longer commercially available, requiring the development of an alternative approach for measuring activity *in vitro*. We adapted the commercially available IP-One assay, typically used to measure G_q signaling in cells, to measure phosphatidylinositol hydrolysis by PLCβ3 *in vitro*. Using this approach, together with thermal stability studies, and liposome binding assays, we found that reversal of charge in the acidic stretch decreased stability, increased activity, but had no impact on liposome binding. Charge reversal of the basic residues on the predicted membrane-facing surface of the TIM barrel also decreased thermal stability, but had no impact on activity or liposome binding. However, when the charge reversal mutations were combined, lipase activity was restored to wild-type basal levels despite a marked increase in liposome binding. Taken together, these studies are consistent with a model wherein intramolecular electrostatic interactions between the acidic stretch of the X–Y linker and the PLCβ3 core directly contribute to autoinhibition.

Materials and Methods

Cloning, expression, and purification of PLCβ3 variants

PLCβ3 (UniProt entry Q01970), PLCβ3-Δ892, and PLCβ3-Δ847 were cloned, expressed, and purified as previously described[19]. PLCβ3-Δ847 mutants were generated using QuikChange (Stratagene, San Diego, CA) or Q5 site-directed mutagenesis (New England Biolabs, Ipswich, MA). All mutations were sequenced over the open reading frame. PLCβ3-Δ847 charge reversal mutants were expressed and purified as previously described[19]. As an additional control, a charge neutral PLCβ3-Δ847 variant was also generated, wherein the

residues of the acidic stretch were mutated to alanine. However, efforts to express and purify this variant to homogeneity were unsuccessful.

Basal activity assays

PIP_2 hydrolysis by PLCβ3 variants was measured as previously described [19, 22]. PLCβ3 was assayed at final concentrations of 2 or 0.5 ng/μL, PLCβ3-Δ892 at 12 ng/μL, and PLCβ3Δ847 at 4 or 5 ng/μL. All assays were performed at least in duplicate with protein from at least two independent purifications.

PI hydrolysis was measured using a modified version of the commercially available IP-One assay (IP-One G_q Kit, Cisbio, Bedford, MA). 100 μM hen egg white phosphatidylethanolamine and 250 μM soy phosphatidylinositol (Avanti Polar Lipids, Alabaster, AL) were mixed and dried under nitrogen. Lipids were resuspended in sonication buffer (50 mM HEPES pH 7.0, 80 mM KCl, 3 mM EGTA, and 1 mM DTT) and sonicated. Assays contained 50 mM HEPES, pH 7, 80 mM KCl, 16.67 mM NaCl, 0.83 mM MgCl, 3 mM DTT, 1 mg/mL BSA, 2.26 mM free Ca^{2+}, and varying amounts of PLCβ3 variant proteins. Protein concentrations were chosen to have activity in the linear range over a 2–10 min time course. The final concentrations used were 20 ng/μL PLCβ3 or PLCβ3-Δ892, 15 ng/μL PLCβ3-Δ847, 0.25 ng/μL PLCβ3-Δ847 E556–566K, 8 ng/μL PLCβ3-Δ847 K601–624E, 4 ng/μL PLCβ3-Δ847 K367–624E, and 4 ng/μL PLCβ3-Δ847 E556–566K/K601–624E. Control reactions contained the same components, but lacked $CaCl_2$. Reactions were initiated by addition of liposomes and transfer to 37 °C. Reactions were quenched upon addition of 5 μL quench buffer (100 mM HEPES pH 7, 160 mM KCl, 1 mM DTT, 210 mM EGTA), and 14 μL of each reaction was then transferred to a 384-well plate (Greiner Bio-One). For IP detection, D_2-labeled IP_1 (fluorescence acceptor) and anti-IP_1 cryptate (fluorescence donor) were pre-incubated with Detection Buffer (Cisbio) and filtered through a 0.2 μm filter (Millipore). 3 μL of D_2-labeled IP_1 and 3 μL anti-IP_1 cryptate were then added to each well used in the 384-well plate. Positive assay controls contained 50 mM HEPES, pH 7, 80 mM KCl, 16.67 mM NaCl, 0.83 mM MgCl, 3 mM DTT, 1 mg/mL BSA, 2.26 mM free Ca^{2+}, D_2-labeled IP_1, and anti-IP_1 cryptate, while negative assay controls contained all components except D_2-labeled IP_1. The plate was then incubated for 1 h in the dark at room temperature, followed by centrifugation at 1,000 × g for 1 min. Plates were read with a Synergy 4 plate reader (BioTek) at 620 and 665 nm. IP_1 was quantified using a standard curve and data reduction protocol for normalization (Cisbio). Data were plotted and statistics were performed using GraphPad Prism v8.0.

Differential Scanning Fluorimetry

Thermal stability of PLCβ3-Δ847 and mutants was determined as previously described[19]. Samples contained 0.2–0.5 mg/mL of the PLCβ3-Δ847 mutant plus 5 mM $CaCl_2$. All experiments were performed in triplicate from at least two independent protein preparations. Thermal denaturation curves were fit to a Boltzman sigmoidal function, and the T_m was calculated from the inflection point (GraphPad Prism 8.0).

Liposome binding assays

PLCβ3-Δ847 variant binding to PE:PIP_2 liposomes was performed as previously described[23], with some modifications. Briefly, 200 μM hen egg white phosphatidylethanolamine and 100 μM porcine brain phosphatidylinositol 4,5-bisphosphate (Avanti Polar Lipids) was mixed and dried under N_2. Lipids were resuspended in 312 μL sonication buffer (50 mM HEPES, pH 7, 80 mM KCl, 3 mM EGTA, and 1 mM DTT), and sonicated. 125 pmol of each PLCβ3-Δ847 variant was incubated with 65 μL of PE:PIP_2 liposomes and sonication buffer in a final volume of 100 μL. Control samples contained protein and buffer only. Samples were incubated for 1 h on ice, then centrifuged at 119,000 x g for 1 h at 4 °C. The supernatant was transferred to a 1.7 mL microfuge tube, the remaining pellet was resuspended in 100 mL sonication buffer, and all samples were stored on ice. 16 μL of the supernatant or resuspended pellet was then denatured with 4 μL of 5X SDS loading dye, and 5 μL of this total sample analyzed by SDS-PAGE. All gels were stained with Bio-Safe Coomassie (Bio-Rad), and band density was quantified with ImageJ and normalized to controls. Each variant was examined at least three times from two different protein preparations.

Statistical Methods

All graphical plots were generated using GraphPad Prism v.8.0. One-way ANOVA was performed with Prism 8.0 and followed by Tukey post-hoc multiple comparisons as noted in figure captions. Error bars represent standard deviation.

Results

Charge reversal mutations in the X–Y linker and the TIM barrel decrease thermal stability

If the acidic stretch in the linker interacts with basic patches on the TIM barrel domain, then the thermal stability of the protein would decrease when the interaction is disrupted, such as by charge reversal mutations. To test this hypothesis, site-directed mutations were introduced in the background of PLCβ3-Δ847, a C-terminal truncation of PLCβ3 that has been previously used to investigate autoinhibition and lacks the regulatory proximal and distal CTDs that would confound analysis (Figure 1). First, the eleven aspartic and glutamic acid residues in the acidic stretch were all converted to lysine to create PLCβ3-Δ847 E556–566K (Table 1), and its thermal stability compared to that of PLCβ3-Δ847 using differential scanning fluorimetry (DSF)[24]. PLCβ3-Δ847 (referred to as WT) has a melting temperature (T_m) of 54.6 ± 0.3 °C, while the T_m of PLCβ3-Δ847 E556–566K was decreased to 53.3 ± 0.6 °C (Figure 2, Table 2).

The surface of the TIM barrel domain features conserved, basic residues predicted to be in close proximity to the acidic stretch of the X–Y linker (Figure 1)[1, 3]. To determine whether these basic residues contribute to thermal stability, two charge reversal mutations were generated. PLCβ3-Δ847 K601–624E and PLCβ3-Δ847 K367–624E (Table 1), convert four or seven residues to glutamates, respectively, that are in close proximity to the C-terminus of the X–Y linker acidic stretch based on crystal structures (Figure 1A,C)[1, 3]. While all of these residues are solvent-exposed, two (K420 and R611) form electrostatic interactions with acidic residues in close proximity, thereby contributing to the tertiary structure of the TIM

barrel. However, both variants were properly folded as assessed by size exclusion chromatography, demonstrating the mutations do not compromise the structure. We found that PLCβ3-Δ847 K601–624E had a T_m of 48.9 ± 2.4 °C, ~6 °C lower than WT. PLCβ3-Δ847 K367-K624E was further destabilized, with a T_m of 45.7 ± 0.4 °C, ~9 °C lower than WT (Figure 2, Table 2). If the loss of thermal stability reflects a loss of favorable electrostatic interactions between the linker and the TIM barrel, then charge reversal mutations in both the acidic stretch and the TIM barrel domain (PLCβ3-Δ847 E556–566K/K601–624E, Table 1) should restore stability. However, this variant had a T_m of 46.5 ± 1.6 °C. Thus, even a variant with the combined charge reversal mutation was destabilized ~7 °C relative to WT (Figure 2, Table 2).

PLCβ3 variants hydrolyze PIP_2 and PI in vitro

The gold-standard assay for measuring *in vitro* PLCβ basal activity has been a liposome-based activity assay, wherein [^{3}H]-PIP_2 is incorporated into liposomes. Following incubation with enzyme, free [^{3}H]-IP_3 is quantified by scintillation counting[22]. However, this critical radiolabelled substrate is no longer commercially available, necessitating the development of an alternative assay for measuring *in vitro* PLCβ activity. PLC enzymes are known to hydrolyze other phosphatidylinositols, including PI, albeit with reduced specific activity[25]. Thus, we turned to the IP-One assay (CisBio, Bedford, MA), which is a well-established method for measuring IP_1 accumulation in cells following stimulation of G_q-coupled receptors. This assay relies on homogenous time resolved fluorescence (HTRF), wherein the fluorescent donor and acceptor interact and emit baseline fluorescence. Upon PIP_2 hydrolysis, IP_3 is produced and is rapidly degraded to IP_1. As IP_1 accumulates in the cell, it binds the fluorescent donor, displacing the acceptor and decreasing the total fluorescence[26, 27].

We expressed and purified full-length PLCβ3 and two previously characterized C-terminal truncations, PLCβ3-Δ847 and PLCβ3-Δ892, and compared their ability to hydrolyze [^{3}H]-PIP_2 versus PI using *in vitro* liposome-based activity assays. [^{3}H]-PIP_2 hydrolysis was measured using well-established protocols[18, 19, 22]. For PI hydrolysis, PI was incorporated into liposomes with phosphatidylethanolamine (PE), using an analogous method as the PIP_2 hydrolysis assay[18, 19, 22]. In both assays, PLCβ3 variants were incubated with the substrate liposomes for increasing times in the presence of ~200 nM free Ca^{2+}, while control assays lacked Ca^{2+}[22]. [^{3}H]-IP_3 was quantified by scintillation counting, whereas *in vitro* IP accumulation was measured by monitoring the change in fluorescence as a function of time, with the final concentration of IP quantified using a standard curve[26, 27]. All three PLCβ3 variants were able to hydrolyze [^{3}H]-PIP_2 or PI under the experimental conditions (Figure 3). Full-length PLCβ3 has the highest activity with both substrates, compared to PLCβ3-Δ892, consistent with the presence of the distal CTD[5]. When PIP_2 is the substrate, PLCβ3 has a specific activity is 37.1 ± 10.5 nmol IP_3/min/nmol enzyme, similar to previous reports[11], versus 0.14 ± 0.05 nmol IP_1/min/nmol enzyme when PI is the substrate. PLCβ3-Δ847 has significantly higher basal activity than PLCβ3-Δ892 whether PIP_2 or PI is used as the substrate (Figure 3)[11, 18]. Finally, the specific activity of PLCβ3-Δ892 is decreased ~4-fold when PI is the substrate, compared to PIP_2 (Figure 3). Thus, although the PLCβ3

variant specific activities are decreased with the PI substrate, the IP-One assay is a viable approach for measuring for measuring PLCβ3 activity *in vitro*.

Charge reversal mutations modulate basal activity

Prior reports suggest that destabilization may contribute to activation of PLCβ[18]. To determine whether destabilization caused by the charge reversal mutations similarly releases autoinhibition, the basal activity of all PLCβ3-Δ847 variants was measured using PI hydrolysis. PLCβ3-Δ847 had a specific activity of 0.14 ± 0.03 nmol IP/min/nmol enzyme (Figure 4, Table 2). The specific activity of PLCβ3-Δ847 E556–566K was 8.9 ± 2.3 nmol IP/min/nmol enzyme, a ~64-fold increase compared to WT PLCβ3-Δ847, and consistent with the acidic stretch being required for autoinhibition. This is comparable to the reported ~30-fold increase in lipase activity when the entire X–Y linker was deleted in PLCβ3-Δ847[18].

In contrast, mutation of the basic TIM barrel surface (PLCβ3-Δ847 K601–624E and PLCβ3-Δ847 K367–624E) had no significant impact on basal activity. Combining the charge reversal mutants in PLCβ3-Δ847 E556–566K/K601–624E also resulted in specific activity similar to the WT protein (Figure 4, Table 2). As mutations to the TIM barrel decrease activity and thermal stability, it may be that the electrostatic properties of this domain are critical for normal function.

PLCβ3-Δ847 charge reversal variants have altered liposome binding

PLCβ3 must associate with the cell membrane in order to hydrolyze its substrate, and alteration of the electrostatic surface perturbs activity and stability. To investigate whether these mutations also perturb the ability of the enzyme to bind to liposomes, a pull-down assay was used to monitor the binding of the PLCβ3-Δ847 variants to PE:PIP_2 liposomes[23, 28]. PLCβ3-Δ847 lacks the distal CTD, which is required for maximum membrane binding, and thus would be expected to bind only weakly to PE:PIP_2 liposomes. As expected, the majority of this protein is present in the supernatant fraction following incubation with PE:PIP_2 liposomes. There is a band present in the pellet fraction, consistent with modest liposome binding and the low basal activity of this variant (Figure 5) [4, 12, 19]. Similarly, mutation of the acidic stretch to polylysine in PLCβ3-Δ847 E556–566K had no impact on liposome binding, with the majority of the protein present in the supernatant. Thus, the increased basal activity of this variant is not due to increased interactions with liposomes (Figure 5).

The ability of the PLCβ3-Δ847 TIM barrel charge reversal mutants to bind the PE:PIP_2 liposomes was then tested. While the basic residues on the TIM barrel surface are not anticipated to contribute to liposome binding, as evidenced by these variants having basal activity comparable to WT, the primary membrane binding surface of PLCβ3 has not yet been experimentally validated[18, 19]. PLCβ3-Δ847 K601–624E and PLCβ3-Δ847 K367–624E were both found primarily in the supernatant after incubation with liposomes (Figure 5), confirming these basic surfaces are not directly involved in liposome binding.

Lastly, PLCβ3-Δ847 E556–566K/K601–624E was assessed for its ability to bind liposomes. Surprisingly, this mutant was found predominantly in the pellet after incubation with

liposomes. This result cannot be attributed to charge reversal of the X–Y linker, as PLCβ3-Δ847 E556–566K interacted with liposomes to a similar extent as PLCβ3-Δ847 (Figure 5). This increased binding also cannot be due to increased interactions between the active site and the liposome, as PLCβ3-Δ847 E556–566K/K601–624E has basal activity comparable to WT (Table 2). These results suggest that introduction of compensatory acidic mutations to the TIM barrel surface, in the presence of the basic X–Y linker, are sufficient to decrease basal activity independently of liposome binding.

Discussion

The poorly conserved X–Y linker is one of the most studied autoinhibitory elements in PLCβ[10, 16–18], but little is known about its mechanism, other than the fact that deletion of the acidic stretch or the entire linker is activating. This has been proposed to be due to elimination of unfavorable charge-charge interactions between the linker and the membrane, which increase substrate binding to the active site[16, 17]. However, crystallization of a PLCβ3 mutant containing a deletion of the acidic stretch revealed that the lid helix becomes disordered in the absence of the acidic stretch[18], suggesting that this region may interact with the TIM barrel to stabilize the conformation of the lid that blocks access to the active site. This indicated that interfacial activation is more complex than simple modulation of charge-charge interactions.

In this work, site-directed mutagenesis was used to investigate whether electrostatic interactions between the X–Y linker and the catalytic TIM barrel domain contribute to PLCβ3 regulation. Mutation of the acidic stretch to polylysine (PLCβ3-Δ847 E556–566K) did not alter thermal stability relative to PLCβ3-Δ847, suggesting that regions of the linker flanking the acidic stretch are important for maintaining stability (Figure 2, Table 2). However, these mutations increased basal activity ~60-fold without appearing to increase binding to negatively charged liposomes (Figure 4,5, Table 2). The latter is surprising given the activity of this mutant and the more complementary charge of the linker with the liposome. One possible explanation is that PIP_2 was depleted from the liposome over the time course of the experiment (1 h), decreasing the negative charge of the liposome and therefore binding[19, 21]. We then introduced charge reversal mutations on the surface of the TIM barrel domain (PLCβ3-Δ847 K637–624E and PLCβ3-Δ847 K601–624E). These variants had decreased stability, but no significant change in activity or association with liposomes (Figure 2, 4, 5). The PLCβ3 crystal structure (PDB ID 3OHM[3]), reveals that K420 and R611 form electrostatic interactions with E373 and E616, respectively, within the TIM barrel. Disruption of interactions such as these may contribute to the ~5–7 °C decrease in stability of these variants. In addition, introduction of negatively charged residues on the TIM barrel surface introduce unfavorable electrostatic interactions with the membrane, leading to reduced activity even if the X–Y linker has been displaced (Figures 1, 2, Table 2). In support of these ideas, the charge-swapped mutant, PLCβ3-Δ847 E556–566K/K601–624E, was less stable than PLCβ3-Δ847, but as predicted, had comparable basal activity (Figure 2, 4, 5, Table 2). Surprisingly, this was the only variant that strongly bound to liposomes (Figure 5).

Overall, these studies emphasize that membrane binding does not always correlate with activity in this system. PLCβ3-Δ847 variants containing charge reversal mutations on the TIM barrel domain all have decreased thermal stability. Furthermore, with the exception of the combined charge reversal mutant (PLCβ3-Δ847 E556–566K/K601–624E), they did not bind liposomes. These trends may have a dominant effect on activity independently of whether the lid helix of the X–Y linker is bound near the active site or not. Overall, the presence of a net negative charge, whether in the acidic stretch of the X–Y linker or on the surface of the TIM barrel is detrimental. However, these results paint a mixed picture as to whether or not interactions between the X–Y linker and the surface of the PLCβ3 core are responsible for autoinhibition. Based on our results, it is likely that the membrane, the X–Y linker, and the TIM barrel interact in a more complex way than previously understood that is difficult to deconvolute (Figure 6). In the future, it would be interesting to look at how X–Y linker reversal affects activation by G proteins, and if the TIM barrel charge reversal mutants can still be activated by the Gβγ heterodimer. In addition, the X–Y linker is also found in the PLCδ, PLCε, and PLCζ subfamilies[17]. In the PLCζ subfamily, the X–Y linker contains a highly basic region, which is proposed to contribute to membrane binding, consistent with our double charge swapped variant. This basic region was shown to preferentially interact with model membranes containing PIP_2[29]. Thus, it appears that the highly-charged character of the X–Y linker is primarily responsible for regulation mediated by this element. However, future studies are also needed to confirm whether the charged nature of the X–Y linker is required for regulation in other subfamilies.

With respect to the charge reversal mutations in PLCβ3 described in this study, perturbation of the electrostatic surfaces on PLCβ would be expected to have profound consequences on downstream processes. For example PLCβ contributes to glucose-stimulated insulin secretion in pancreatic β-cells[30]. Following activation by $G\alpha_q$, the increased PIP_2 hydrolysis by PLCβ stimulates intracellular Ca^{2+} release, facilitates opening of store-operated channels (SOC) that conduct Ca^{2+} and some transient receptor potential (TRP) channels, including TRPC3[31]. In addition to second messenger production at the plasma membrane, PLCβ activity in the nucleus is also essential for maintaining normal β-cell function[32–35].There, PLCβ activity upregulates expression of genes involved in insulin secretion, including PPAR-γ (peroxisome proliferator-activated receptor γ)[36, 37] (Figure 7A). Loss of the acidic stretch would lead to constitutive activity, leading to depletion of PIP_2 and dampening of Ca^{2+} oscillations. Although this mutant would retain the ability to bind activated $G\alpha_q$, the Ca^{2+} oscillations required for insulin secretion would be uncoupled from extracellular signals. Finally, the depletion of PIP_2 in the cell would likely alter nuclear PLCβ activity and the expression of insulin sensing and secreting genes. The changes in PIP_2 levels would also alter other pathways that rely on the balance of phosphatidylinositides in cellular membranes (Figure 7B)[38].

Finally, this study required the development of a new method for measuring *in vitro* PLC activity. The gold-standard assay in the field has long been the hydrolysis of [^{3}H]-PIP_2 from liposomes[22]. However, this critical reagent is no longer commercially available, and custom biosynthesis of the lipid is prohibitively expensive. To circumvent this problem, we turned to the commercially available IP-One assay, which is routinely used to measure IP accumulation in cells following stimulation of Gq-coupled GPCRs[26, 39]. PLC enzymes can

hydrolyze other phosphatidylinositol species *in vitro* and in cells[25, 40, 41], thus PLC-dependent hydrolysis of PI hydrolysis could be detected and quantified. Using human PLCβ3 and two previously characterized C-terminal truncations, we demonstrated that these proteins can hydrolyze PI from liposomes under the same conditions as [^{3}H]-PIP_2 (Figure 3). These proteins also showed similar trends in specific activity with both substrates (Figure 3). Thus, the IP-One assay, modified to measure liposome-based PI hydrolysis, is a valid method for measuring *in vitro* PLC activity.

Acknowledgement

We thank Osvaldo Cruz-Rodriguez (University of Michigan) for technical assistance with the IP-One assay. This work was supported by an NIH 1R01HL141076–01, American Heart Association Scientist Development Grant 16SDG29930017, and an American Cancer Society Institutional Research Grant (IRG-14–190-56) to the Purdue University Center for Cancer Research (A.M.L). The content is solely the responsibility of the authors and does not necessarily reflect the official views of the National Heart, Lung, and Blood Institute, or the National Institutes of Health.

Funding Sources

This work was supported by an NIH 1R01HL141076–01 (A.M.L.), American Heart Association Scientist Development Grant 16SDG29930017 to A.M.L., and an American Cancer Society Institutional Research Grant (IRG-14–190-56) to the Purdue University Center for Cancer Research (A.M.L).

Abbreviations

PLC	Phospholipase C
PIP_2	phosphatidylinositol-4,5-bisphosphate
IP_3	inositol-1,4,5-triphopshate
DAG	diacylglycerol
Ca^{2+}	calcium
GPCR	G protein-coupled receptor
PE	phosphatidylethanolamine
PIP	phosphatidylinositol phosphate
IP_1	inositol phosphate
DSF	differential scanning fluorimetry

References

[1]. Jezyk MR, Snyder JT, Gershberg S, Worthylake DK, Harden TK, and Sondek J (2006) Crystal structure of Rac1 bound to its effector phospholipase C-β2, Nat Struct Mol Biol 13, 1135–1140. [PubMed: 17115053]

[2]. Dolinsky TJ, Nielsen JE, McCammon JA, and Baker NA (2004) PDB2PQR: an automated pipeline for the setup of Poisson-Boltzmann electrostatics calculations, Nucleic Acids Res 32, W665–667. [PubMed: 15215472]

[3]. Waldo GL, Ricks TK, Hicks SN, Cheever ML, Kawano T, Tsuboi K, Wang X, Montell C, Kozasa T, Sondek J, and Harden TK (2010) Kinetic scaffolding mediated by a phospholipase C-β and G_q signaling complex, Science 330, 974–980. [PubMed: 20966218]

[4]. Kadamur G, and Ross EM (2013) Mammalian phospholipase C, Annu Rev Physiol 75, 127–154. [PubMed: 23140367]

[5]. Lyon AM, and Tesmer JJ (2013) Structural Insights into Phospholipase C-beta Function, Mol Pharmacol 84, 488–500. [PubMed: 23880553]

[6]. Filtz TM, Grubb DR, McLeod-Dryden TJ, Luo J, and Woodcock EA (2009) G_q-initiated cardiomyocyte hypertrophy is mediated by phospholipase Cβ1b, FASEB J 23, 3564–3570. [PubMed: 19564249]

[7]. Grubb DR, Crook B, Ma Y, Luo J, Qian HW, Gao XM, Kiriazis H, Du XJ, Gregorevic P, and Woodcock EA (2015) The atypical 'b' splice variant of phospholipase Cbeta1 promotes cardiac contractile dysfunction, J Mol Cell Cardiol 84, 95–103. [PubMed: 25918049]

[8]. Dent MR, Dhalla NS, and Tappia PS (2004) Phospholipase C gene expression, protein content, and activities in cardiac hypertrophy and heart failure due to volume overload, Am J Physiol Heart Circ Physiol 287, H719–727. [PubMed: 15072958]

[9]. Gresset A, Sondek J, and Harden TK (2012) The phospholipase C isozymes and their regulation, Subcell Biochem 58, 61–94. [PubMed: 22403074]

[10]. Zhang W, and Neer EJ (2001) Reassembly of phospholipase C-β2 from separated domains: analysis of basal and G protein-stimulated activities, J Biol Chem 276, 2503–2508. [PubMed: 11044443]

[11]. Lyon AM, Tesmer VM, Dhamsania VD, Thal DM, Gutierrez J, Chowdhury S, Suddala KC, Northup JK, and Tesmer JJ (2011) An autoinhibitory helix in the C-terminal region of phospholipase C-β mediates $G\alpha_q$ activation, Nat Struct Mol Biol 18, 999–1005. [PubMed: 21822282]

[12]. Kim CG, Park D, and Rhee SG (1996) The role of carboxyl-terminal basic amino acids in $G_q\alpha$-dependent activation, particulate association, and nuclear localization of phospholipase C-β1, J Biol Chem 271, 21187–21192. [PubMed: 8702889]

[13]. Ilkaeva O, Kinch LN, Paulssen RH, and Ross EM (2002) Mutations in the carboxyl-terminal domain of phospholipase Cβ 1 delineate the dimer interface and a potential $G\alpha_q$ interaction site, J Biol Chem 277, 4294–4300. [PubMed: 11729196]

[14]. Lyon AM, Dutta S, Boguth CA, Skiniotis G, and Tesmer JJ (2013) Full-length Galpha(q)-phospholipase C-beta3 structure reveals interfaces of the C-terminal coiled-coil domain, Nat Struct Mol Biol 20, 355–362. [PubMed: 23377541]

[15]. Singer AU, Waldo GL, Harden TK, and Sondek J (2002) A unique fold of phospholipase C-β mediates dimerization and interaction with $G\alpha_q$, Nature structural biology 9, 32–36. [PubMed: 11753430]

[16]. Charpentier TH, Waldo GL, Barrett MO, Huang W, Zhang Q, Harden TK, and Sondek J (2014) Membrane-induced allosteric control of phospholipase C-beta isozymes, J Biol Chem 289, 29545–29557. [PubMed: 25193662]

[17]. Hicks SN, Jezyk MR, Gershburg S, Seifert JP, Harden TK, and Sondek J (2008) General and versatile autoinhibition of PLC isozymes, Mol Cell 31, 383–394. [PubMed: 18691970]

[18]. Lyon AM, Begley JA, Manett TD, and Tesmer JJ (2014) Molecular Mechanisms of Phospholipase C beta3 Autoinhibition, Structure 22, 1844–1854. [PubMed: 25435326]

[19]. Hudson BN, Hyun SH, Thompson DH, and Lyon AM (2017) Phospholipase Cbeta3 Membrane Adsorption and Activation Are Regulated by Its C-Terminal Domains and Phosphatidylinositol 4,5-Bisphosphate, Biochemistry 56, 5604–5614. [PubMed: 28945350]

[20]. Adjobo-Hermans MJ, Crosby KC, Putyrski M, Bhageloe A, van Weeren L, Schultz C, Goedhart J, and Gadella TW Jr. (2013) PLCβ isoforms differ in their subcellular location and their CT-domain dependent interaction with $G\alpha_q$, Cell Signal 25, 255–263. [PubMed: 23006664]

[21]. Adjobo-Hermans MJ, Goedhart J, and Gadella TW Jr. (2008) Regulation of PLCβ1a membrane anchoring by its substrate phosphatidylinositol (4,5)-bisphosphate, J Cell Sci 121, 3770–3777. [PubMed: 18957514]

[22]. Ghosh M, and Smrcka AV (2004) Assay for G protein-dependent activation of phospholipase C β using purified protein components, Methods Mol Biol 237, 67–75. [PubMed: 14501039]

[23]. Garland-Kuntz EE, Vago FS, Sieng M, Van Camp M, Chakravarthy S, Blaine A, Corpstein C, Jiang W, and Lyon AM (2018) Direct observation of conformational dynamics of the PH domain in phospholipases C and beta may contribute to subfamily-specific roles in regulation, J Biol Chem 293, 17477–17490. [PubMed: 30242131]

[24]. Mezzasalma TM, Kranz JK, Chan W, Struble GT, Schalk-Hihi C, Deckman IC, Springer BA, and Todd MJ (2007) Enhancing recombinant protein quality and yield by protein stability profiling, J Biomol Screen 12, 418–428. [PubMed: 17438070]

[25]. Ellis MV, James SR, Perisic O, Downes CP, Williams RL, and Katan M (1998) Catalytic domain of phosphoinositide-specific phospholipase C (PLC). Mutational analysis of residues within the active site and hydrophobic ridge of PLCδ1, J Biol Chem 273, 11650–11659. [PubMed: 9565585]

[26]. Trinquet E, Fink M, Bazin H, Grillet F, Maurin F, Bourrier E, Ansanay H, Leroy C, Michaud A, Durroux T, Maurel D, Malhaire F, Goudet C, Pin JP, Naval M, Hernout O, Chretien F, Chapleur Y, and Mathis G (2006) D-myo-inositol 1-phosphate as a surrogate of D-myo-inositol 1,4,5-tris phosphate to monitor G protein-coupled receptor activation, Anal Biochem 358, 126–135. [PubMed: 16965760]

[27]. Ryu SH, Suh PG, Cho KS, Lee KY, and Rhee SG (1987) Bovine brain cytosol contains three immunologically distinct forms of inositolphospholipid-specific phospholipase C, Proc Natl Acad Sci U S A 84, 6649–6653. [PubMed: 3477795]

[28]. Glukhova A, Hinkovska-Galcheva V, Kelly R, Abe A, Shayman JA, and Tesmer JJ (2015) Structure and function of lysosomal phospholipase A2 and lecithin:cholesterol acyltransferase, Nat Commun 6, 6250. [PubMed: 25727495]

[29]. Nomikos M, Mulgrew-Nesbitt A, Pallavi P, Mihalyne G, Zaitseva I, Swann K, Lai FA, Murray D, and McLaughlin S (2007) Binding of phosphoinositide-specific phospholipase C-zeta (PLC-zeta) to phospholipid membranes: potential role of an unstructured cluster of basic residues, J Biol Chem 282, 16644–16653. [PubMed: 17430887]

[30]. Hwang HJ, Jang HJ, Cocco L, and Suh PG (2019) The regulation of insulin secretion via phosphoinositide-specific phospholipase Cbeta signaling, Advances in biological regulation 71, 10–18. [PubMed: 30293894]

[31]. Xie LH, Horie M, and Takano M (1999) Phospholipase C-linked receptors regulate the ATP-sensitive potassium channel by means of phosphatidylinositol 4,5-bisphosphate metabolism, Proc Natl Acad Sci U S A 96, 15292–15297. [PubMed: 10611378]

[32]. Crowder MK, Seacrist CD, and Blind RD (2017) Phospholipid regulation of the nuclear receptor superfamily, Advances in biological regulation 63, 6–14. [PubMed: 27838257]

[33]. Cocco L, Follo MY, Faenza I, Billi AM, Ramazzotti G, Martelli AM, Manzoli L, and Weber G (2010) Inositide signaling in the nucleus: from physiology to pathology, Adv Enzyme Regul 50, 2–11. [PubMed: 19895834]

[34]. Fiume R, Keune WJ, Faenza I, Bultsma Y, Ramazzotti G, Jones DR, Martelli AM, Somner L, Follo MY, Divecha N, and Cocco L (2012) Nuclear phosphoinositides: location, regulation and function, Subcell Biochem 59, 335–361. [PubMed: 22374096]

[35]. Jacobsen RG, Mazloumi Gavgani F, Edson AJ, Goris M, Altankhuyag A, and Lewis AE (2019) Polyphosphoinositides in the nucleus: Roadmap of their effectors and mechanisms of interaction, Advances in biological regulation 72, 7–21. [PubMed: 31003946]

[36]. Fiume R, Ramazzotti G, Faenza I, Piazzi M, Bavelloni A, Billi AM, and Cocco L (2012) Nuclear PLCs affect insulin secretion by targeting PPARgamma in pancreatic beta cells, FASEB J 26, 203–210. [PubMed: 21974932]

[37]. Gupta D, Kono T, and Evans-Molina C (2010) The role of peroxisome proliferator-activated receptor gamma in pancreatic beta cell function and survival: therapeutic implications for the treatment of type 2 diabetes mellitus, Diabetes Obes Metab 12, 1036–1047. [PubMed: 20977574]

[38]. Hermida MA, Dinesh Kumar J, and Leslie NR (2017) GSK3 and its interactions with the PI3K/AKT/mTOR signalling network, Advances in biological regulation 65, 5–15. [PubMed: 28712664]

[39]. Zhang JY, Kowal DM, Nawoschik SP, Dunlop J, Pausch MH, and Peri R (2010) Development of an improved IP(1) assay for the characterization of 5-HT(2C) receptor ligands, Assay Drug Dev Technol 8, 106–113. [PubMed: 19922239]

[40]. Nash CA, Brown LM, Malik S, Cheng X, and Smrcka AV (2018) Compartmentalized cyclic nucleotides have opposing effects on regulation of hypertrophic phospholipase Cepsilon signaling in cardiac myocytes, J Mol Cell Cardiol.

[41]. Zhang L, Malik S, Pang J, Wang H, Park KM, Yule DI, Blaxall BC, and Smrcka AV (2013) Phospholipase cepsilon hydrolyzes perinuclear phosphatidylinositol 4-phosphate to regulate cardiac hypertrophy, Cell 153, 216–227. [PubMed: 23540699]

Highlights

- Monitoring PI hydrolysis is a viable method for measuring in vitro activity of PLC.
- PLCβ3 autoinhibition requires a highly negatively charged X–Y linker.
- Intramolecular electrostatics within PLCβ3 regulate its stability and activity.

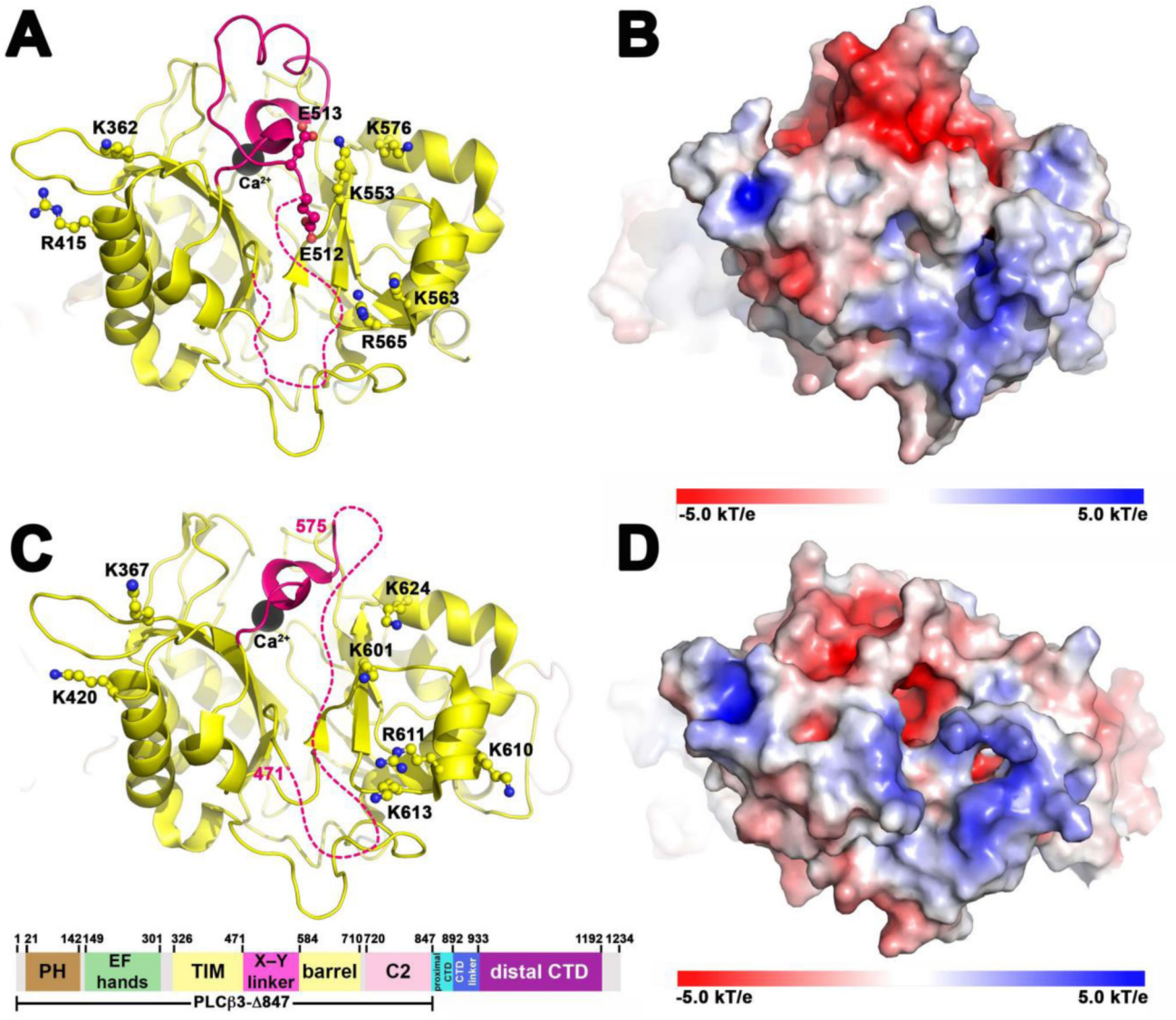

Figure 1.

The PLCβ2 and PLCβ3 X–Y linker and TIM barrel have similar electrostatic properties. (**A**) A crystal structure of PLCβ2 (PDB ID 2FJU[1]) reveals electron density for the last two residues in the acidic stretch shown in ball and stick (E513 and E512) immediately preceding the lid helix (hot pink). The disordered region of the X–Y linker is shown as a dashed line, with the ends denoted by residue number. The TIM barrel domain (yellow) features highly conserved, solvent-exposed, basic residues (shown in ball and stick). The catalytic Ca^{2+} ion is shown as a black sphere. (**B**) Electrostatic surface rendering of (A), wherein positive regions are colored blue and negative regions in red[2]. (**C**) Crystal structure of PLCβ3 (PDB ID 3OHM[3]), shown in the same orientation and coloring as in (A). Shown below the crystal structure is the domain diagram of PLCβ3. Numbers above the diagram corresponds to residues at domain boundaries, and the C-terminal truncation of PLCβ3-Δ847 is shown below. (**D**) Electrostatic surface rendering of (C). In both structures, the basic

surfaces of the TIM barrel domain could favorably interact with the acidic stretch of the X–Y linker.

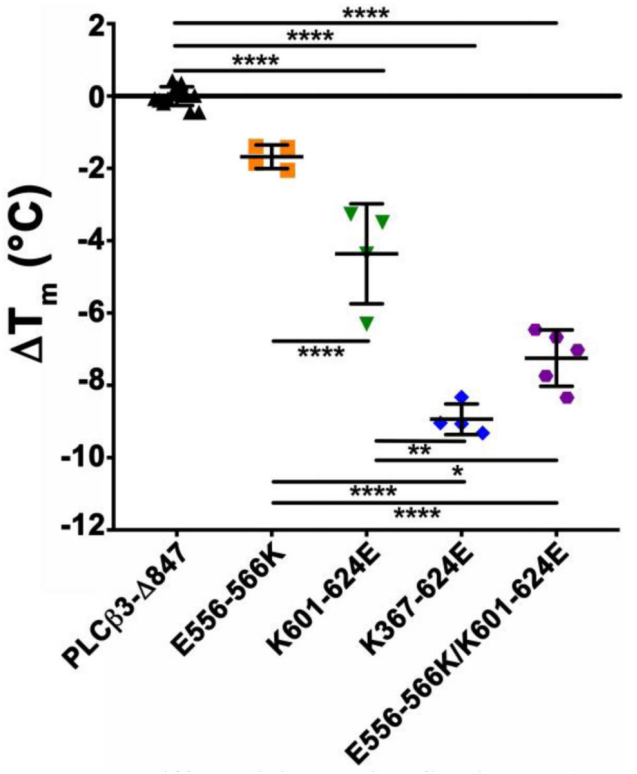

Figure 2.

Differential scanning fluorimetry (DSF) was used to measure the T_m of each PLCβ3-Δ847 charge reversal variant. Mutations within the X–Y linker and/or the TIM barrel domain decrease the T_m of each variant (ΔT_m) relative to PLCβ3-Δ847. Data represent at least two independent experiments measured in triplicate ± SD, from at least two purifications. Significance was determined by one-way ANOVA followed by Tukey's multiple comparison test (****, $p \leq 0.0001$; **, $p \leq 0.0024$; *, $p \leq 0.0113$).

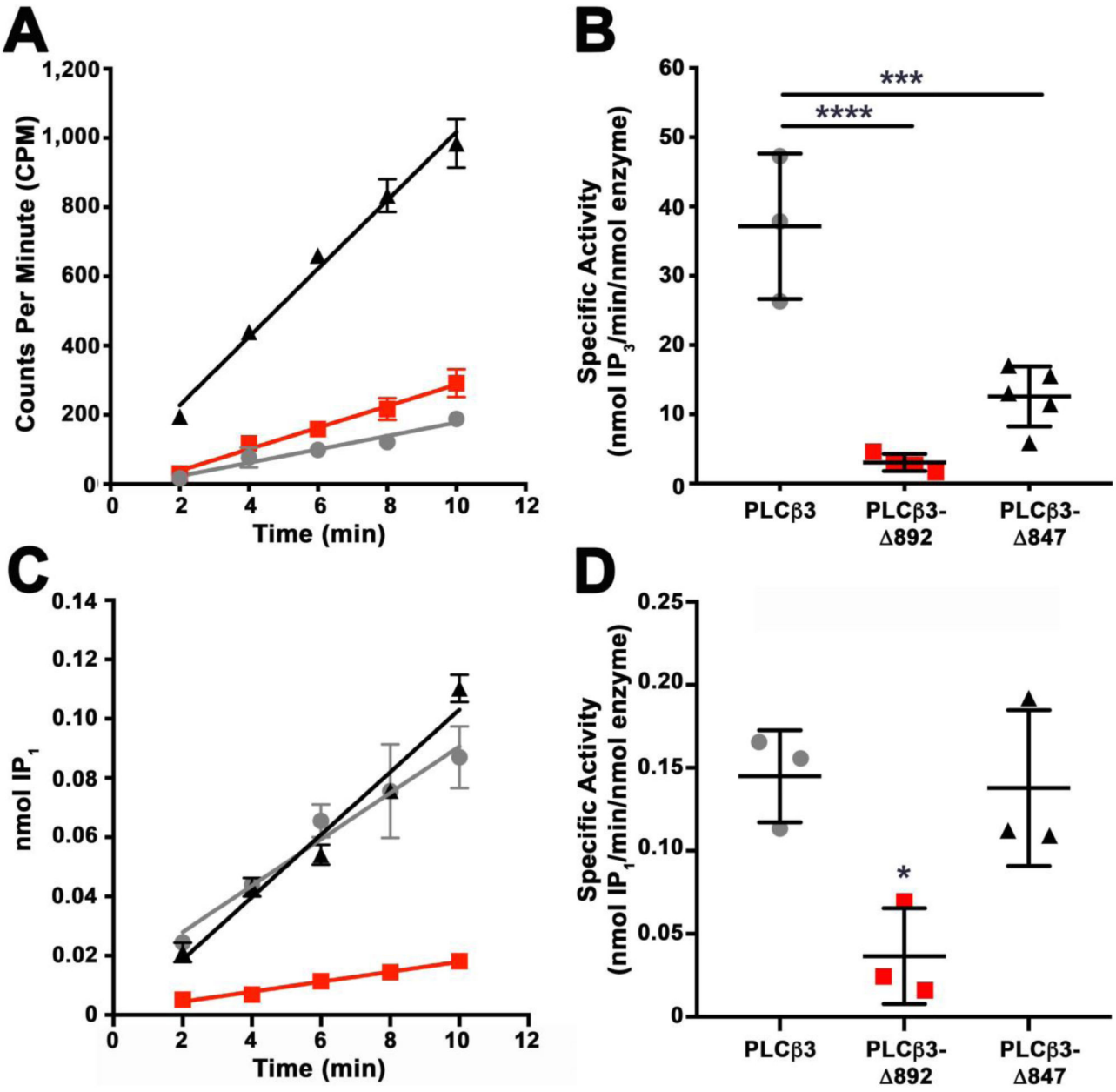

Figure 3.

PLCβ3 variants hydrolyze PIP_2 and PI from liposomes. (A) The ability of PLCβ3 (gray circles), PLCβ3-Δ892 (red squares), and PLCβ3-Δ847 (black triangles) to hydrolyze [^{3}H]-PIP_2 from liposomes was measured as a function of time. (B) The specific activity of PLCβ3 is 37.1 ± 10.5 nmol IP_3/min/nmol enzyme, PLCβ3-Δ892 is 3.0 ± 1.2 nmol IP_3/min/nmol enzyme, and PLCβ3-Δ847 is 13 ± 4.3 nmol IP_3/min/nmol enzyme (****, $p < 0.0001$, ***, $p \leq 0.0007$). (C) The ability of PLCβ3 (gray circles), PLCβ3-Δ892 (red squares), and PLCβ3-Δ847 (black triangles) to hydrolyze PI from liposomes was also measured as a function of time. (D) The specific activity of PLCβ3 is 0.14 ± 0.05 nmol IP_1/min/nmol enzyme, PLCβ3-Δ892 is 0.04 ± 0.03 nmol IP_1/min/nmol enzyme, and PLCβ3-Δ847 is 0.14 ± 0.03 nmol IP_1/min/nmol (*, $p < 0.03$). Data represents the average from at least three independent

experiments in duplicate ± SD. Significance was determined by one-way ANOVA followed by Tukey's multiple comparison test.

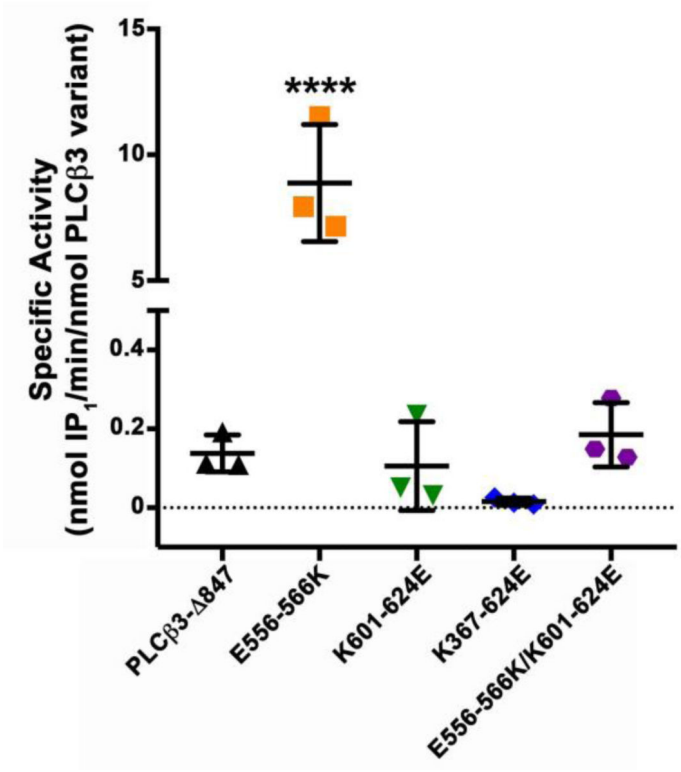

Figure 4.

Mutation of the acidic stretch in the X–Y linker increases enzyme activity. PLCβ3-Δ847 (black triangles) hydrolyzes PI from liposomes with a specific activity of 0.14 ± 0.03 nmol IP_1/min/nmol enzyme. Charge reversal of the X–Y linker in PLCβ3-Δ847 E556–566K (orange squares) significantly increases basal activity (****, $p < 0.0001$). Mutation of the TIM barrel in K601–624E (green inverted triangles) and K367–624E (blue diamonds) has minimal impact on activity. Combining the charge reversal mutations in E556–566K/K601–624E (purple hexagons) does not alter basal activity. Data represents the average from at least three independent experiments in duplicate ± SD. Significance was determined by one-way ANOVA followed by Tukey's multiple comparison test.

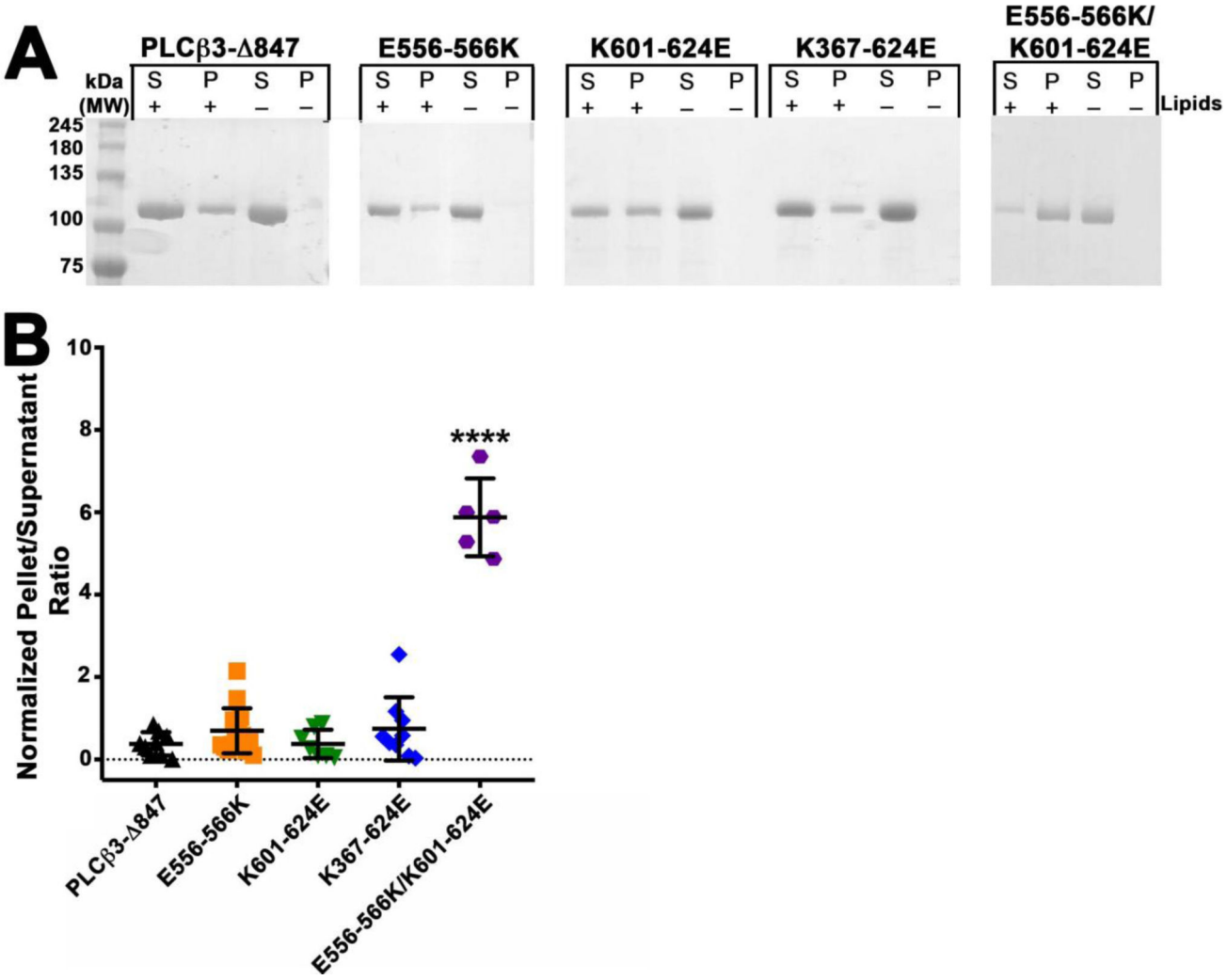

Figure 5.

Charge reversal of the acidic stretch within the X–Y linker and the basic residues on the TIM barrel increase liposome binding. (**A**) Representative SDS-PAGE gels of PLCβ3-Δ847 and charge reversal variants after incubation with (+) PE:PIP_2 liposomes or (−) buffer. Identical volumes of supernatant (S) or resuspended pellet (P) were analyzed for each experiment. White spaces show samples analyzed on different gels. (**B**) The band density of the pellet and supernatant fractions under each condition were quantified using ImageJ. PLCβ3-Δ847 and charge reversal mutants are present primarily in the supernatant following incubation with liposomes, with the exception of the PLCβ3-Δ847 variant, E556–566A/K601–624E, which is present in the pellet after incubation. Data represent at least three independent experiments ± SD. Significance was determined by one-way ANOVA followed by Tukey's multiple comparison test (****, $p \leq 0.0001$).

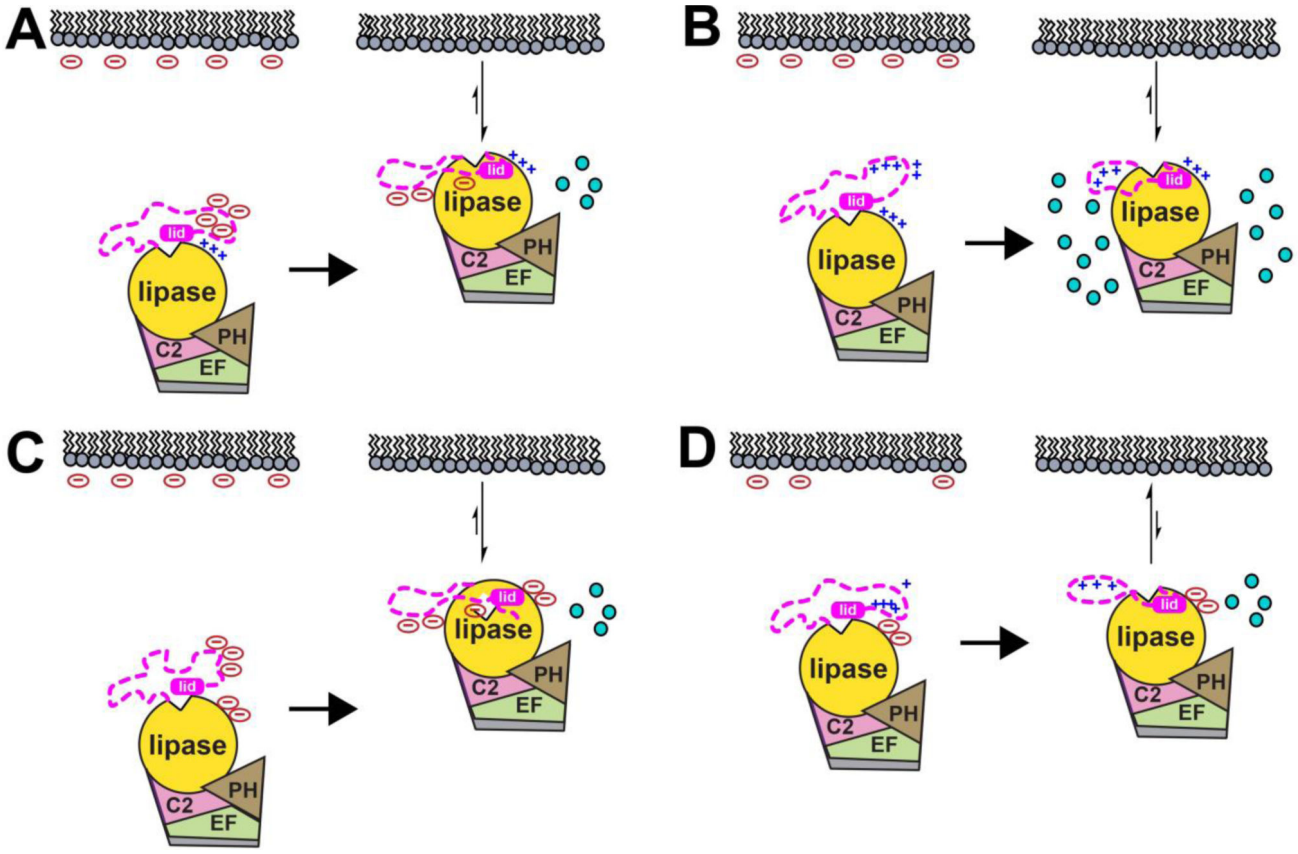

Figure 6.

Intramolecular electrostatic interactions modulate PLCβ3 activity. The electrostatic properties of the X–Y linker and the TIM barrel contribute to activity, stability, and liposome binding. Domains are colored as in Figure 1, with teal circles representing IP_3 produced by PIP_2 hydrolysis. (A) In the wild-type enzyme, the acidic stretch of the X–Y linker (circled minus signs) hinders membrane binding (*right*). Interfacial activation displaces the acidic stretch and lid helix, allowing the active site to bind the negatively charged membrane (circled minus signs), potentially aided by the basic surface of the TIM barrel (blue plus signs) (*left*). (B) Reversing the charge of the acidic stretch to polylysine (*right*) increases basal activity without altering liposome binding (*left*). (C) Reversing the charge of the TIM barrel decreases stability (*right*), but has minimal impact on liposome binding and activity (*left*), likely due to unfavorable electrostatic interactions within the TIM barrel. (D) Reversing the charge of the acidic stretch and the TIM barrel decreases stability (*right*) and increases liposome binding, but has no impact on basal activity (*left*). In this mutant, the X–Y linker could interact with the membrane and/or the TIM barrel.

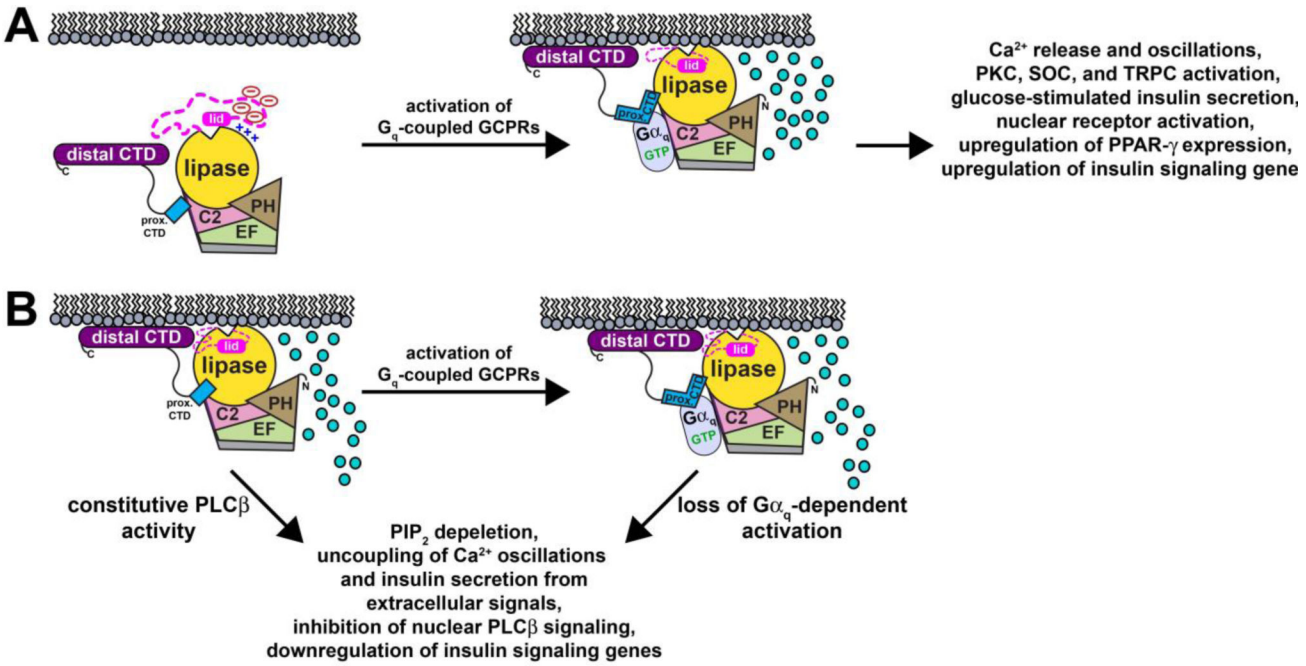

Figure 7.

Potential roles for PLCβ activity in pancreatic β-cells. Domains are colored as in Figure 1, with teal circles representing IP_3 produced by PIP_2 hydrolysis. (A) Following the stimulation of G_q-coupled GPCRs, $G\alpha_q$ binds to PLCβ, stimulating its lipase activity. The increase in the second messengers IP_3 and DAG activating downstream events required for normal insulin secretion, including the induction of Ca^{2+} oscillations, ion channel activation, and nuclear signaling events such as upregulation of PPAR-γ. (B) Electrostatic mutations with PLCβ could result in constitutive membrane association and/or activation. While the mutant PLCβ3 could still bind $G\alpha_q$, the efficacy of activation would be diminished, effectively uncoupling PLCβ activity from extracellular signals. This would result in PIP_2 depletion, uncoupling and dampening of Ca^{2+} oscillations, decreased nuclear PLCβ activity, and downregulation of insulin signaling genes.

Table 1.

PLCβ3-Δ847 Charge Reversal Mutations

Variant	Mutation
PLCβ3-Δ847	*H. sapiens* PLCβ3 residues 10–847
E556–566K[1]	E556K/D557K/E558K/E559K/E560K/D561K/E562K/E563K/E564K/E565K/E566K
K601–624E	K601E/K611E/R613E/K624E
K367–624E	K367E/K420E/K601E/K610E/K611E/R613E/K624E
E556–566K/K601–624E	E556K/D557K/E558K/E559K/E560K/D561K/E562K/E563K/E564K/E565K/E566K/ K601E/K611E/R613E/ K624E

Table 2.

Thermal Stability and Basal Activity of PLCβ3-Δ847 Charge Reversal Mutants

PLCβ3-Δ847 variant	T_m ± SD (°C)	Specific Activity ± SD (nmol IP_1/min/nmol enzyme)
PLCβ3-Δ847 (WT)	54.6 ± 0.3[1]	0.14 ± 0.03
E556–566K	53.3 ± 0.6[2]	8.9 ± 2.3[5]
K601–624E	48.9 ± 2.4[3,4]	0.11 ± 0.1
K367–624E	45.7 ± 0.4	0.016 ± 0.009
E556–566K/K601–624E	46.5 ± 1.6	0.19 ± 0.08

Data represent at least three independent experiments measured in duplicate ± SD, from at least two protein purifications. Significance was determined by one-way ANOVA followed by Tukey's multiple comparison test.

[1] $p \leq 0.0001$, relative to all mutants except PLCβ3-Δ847 E556–566K.

[2] $p \leq 0.0001$, relative to K601–624E and K367–624E, E556–566K/K601–624E

[3] $p \leq 0.0024$ relative to K367–624E

[4] $p \leq 0.0113$ relative to E556–566K/K601–624E

[5] $p \leq 0.0001$ relative to all other mutants